Radar Sensing via Geometric Machine Learning over Riemannian Manifolds

Joarder Jafor Sadique¹, Imtiaz Nasim², and Ahmed S. Ibrahim¹

¹Department of Electrical and Electronic Engineering, Florida International University, Miami, FL 33199, USA

²Idaho National Laboratory, 1955 N Fremont Ave, Idaho Falls, ID 83415, USA

Emails: jsadi004@fiu.edu, imtiaz.nasim@inl.gov, aibrahim@fiu.edu

Abstract—The imperative for autonomously detecting radar signals is paramount in the context of emerging shared-spectrum wireless networks, such as the Citizens Broadband Radio Service (CBRS) band. The dynamic allocation of this spectrum hinges upon a specialized sensor network tasked with identifying the presence of federal incumbent radar signals. In this paper, we propose a radar sensing strategy using received signals at base stations. More specifically, the sample covariance matrices of received signals lie over Riemannian manifolds (i.e., curved surfaces) thanks to their symmetric positive definite (SPD) properties. Consequently, we propose to use support vector machine (SVM) learning models over Riemannian manifolds for classification of radar existence. Our findings reveal that the model attains more than 90% radar detection accuracy considering Signal-to-noise ratio (SNR) values up to 14 dB.

Index Terms—CBRS, machine learning, radar detection, Riemannian manifold, spectrum sensing.

I. INTRODUCTION

In the ever-evolving landscape of wireless communication, incumbent radar bands are finding themselves in new roles as they are shared with commercial mobile broadband systems [1]. This strategic sharing is a move towards optimizing the use of precious radio spectrum resources through dynamic spectrum access. A notable example of this spectrum-sharing paradigm in action is the Citizens Broadband Radio Service (CBRS) band in the United States. CBRS allows for commercial broadband access to the radio frequency spectrum ranging from 3550 MHz to 3700 MHz, and this access is shared with the incumbent users in that frequency band [2]. To decide whether the shared band should be utilized alongside radar, detecting radar signals with complete accuracy is of tremendous importance.

Previously, both model-based and data-based incumbent radar sensing approaches have been observed in literature. In model-based radar sensing, traditional matched-filter detectors showed effective detection results even amidst scenarios involving co-channel interference from commercial users and

This work was supported in part by the National Science Foundation under Award CNS-2144297.

out-of-band emissions emanating from radars in neighboring frequency bands [3]. However, it is worth noting that matched filtering-based detection methods typically rely on having complete or partial information about radar waveforms [4], rendering them unsuitable when the spectrum sensing sensor lacks knowledge of the transmitted signal parameters [1]. For data-based radar sensing, deep learning (DL) techniques have been used such as in [5]-[7]. These works have employed DL techniques for tasks like radar waveform recognition and spectrum allocation in low-interference scenarios within the CBRS. For instance, in [5], authors assessed the performance of different methods related to DL for SPN-43 radar detection using over 14,000 spectrograms collected in the 3.5 GHz band. In [6], a deep convolutional neural network (CNN) based framework was introduced to detect radar radar signals within the radio spectrum, even when they are mixed with interference. Lastly, [7] explored multiple deep learning models for environmental sensing capability (ESC) radar detection.

In recent time, Riemannian geometry has been employed to explore the geometric aspects of second order channel statistics like channel covariance matrix [8], [9] and also wireless link scheduling within device-to-device networks [10], [11]. Radar detection is also done by modeling covariance matrices over Riemannian manifolds, as demonstrated in works such as [12]-[14]. In [12], authors used sample covariance matrices for the radio spectrum sensing. Riemannian distance based detector was proposed in [13] which utilizes wideband spectrum information for sensing. Authors in [14] leveraged K-means clustering technique to address the spectrum sensing problem. Although these works employed Riemannian manifolds, they did not specifically address the unique challenges presented by the 3.5 GHz CBRS band. As the radar parameter varies over a wide range, the radar detection problem becomes more challenging in the CBRS band [4].

In this paper, we model radar sensing over Riemannian manifold in the CBRS band. The concept of harnessing

the inherent geometry of the Riemannian manifold aims to devise computationally efficient on-demand spectrum access strategies. We use sample covariance matrices of the received signals which are represented over Riemannian manifolds due to their symmetric positive definite (SPD) structure. Two signal hypothesises are considered, namely, between radar plus noise versus noise only. Each one of these signals has its own SPD signature, thus we frame the detection challenge as a binary classification task and employ support vector machine (SVM) as a supervised machine learning technique over Riemannian manifold. The proposed SVM has low complexity. To build our model, we utilize the RF dataset comprised of radar waveforms generated synthetically by National Institute of Standards and Technology (NIST) [15]. With the utilization of this dataset, our objective is to train and test the SVM model as a reference point and assess the performance of SVM classifier based on metrics like probability of detection and probability of false alarm.

II. PRELIMINARIES

A. Riemannian Geometry

At any specific point q within a manifold \mathcal{M} , there exists a tangent space denoted as $\mathcal{T}_{\mathbf{q}}\mathcal{M}$, which comprises a set of tangent vectors representing derivatives of curves passing through that particular point. The Riemannian manifold $(\mathcal{M}, \mathcal{L})$ can be described as a real differentiable manifold denoted as \mathcal{M} , in which each tangent space is endowed with an inner product denoted as \mathcal{L} , a Riemannian metric. This metric smoothly varies from one point to another and is the subject of study within the area of Riemannian geometry. Additionally, the $n \times n$ SPD matrices, denoted as Sym_n^{++} , reside within the interior of convex cones, constituting a distinct class of Riemannian manifolds [16].

B. Support Vector Machine

As a supervised machine learning technique, support vector machine (SVM) stands out with its robust method for tackling both classification and regression tasks, aiming to identify the optimal decision boundary in n-dimensional space.

In the context of a Riemannian manifold, the SVM algorithm considers manifold's curvature and finds the optimal separating hyperplane that best divides the classes of data points according to their intrinsic geometric properties. Fig. 1 shows that the SVM classifier divides SPD data points into two classes over Riemannian manifold, \mathcal{M} . One class represents the existence of radar, while the other indicates its absence.

SVM's ability to handle high-dimensional feature spaces makes it an ideal candidate for radar detection applications, where the goal is to effectively differentiate between signal and noise amidst varying environmental conditions. Furthermore, SVM's robustness to outliers and its capacity to incorporate

diverse kernel functions render it adaptable to different radar signal characteristics and deployment scenarios.

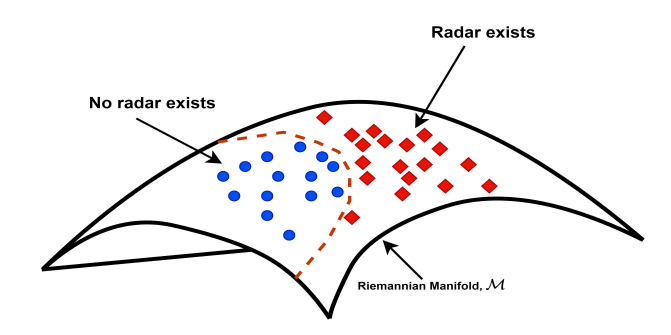


Fig. 1: Classified data points by SVM over Riemannian manifold.

III. SYSTEM MODEL

A. Scenario Description

Fig. 2 provides an overview of the coexistence scenario investigated in this work. It includes established radar systems and commercial broadband base stations sharing the same spectrum, similar to the situation in the CBRS band. Within this setup, active scanning radars, such as those found on ships along coastlines and operated by the military, are employed for target detection. Additionally, the surrounding base stations, including mobile road-side units (RSUs), are equipped with radar sensing capabilities to identify the presence and intensity of radars within their respective coverage areas. In a distributed network, depending on the radar types identified, each base station utilizes the proposed on-demand radar detection strategy to decide whether to access the spectrum or not.

It is assumed that a particular base station in Fig. 2 has M antennas. It is also assumed that the incumbent users (e.g., radars) have N antennas.

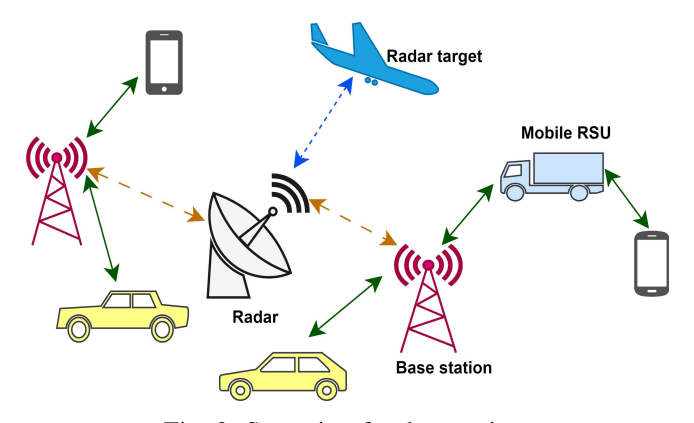


Fig. 2: Scenario of radar sensing.

B. Problem Formulation

With H_0 representing absence of radar (noise only) and H_1 representing presence of radar plus noise, the statistical hypothesis testing used for radar signal detection can be described as follows

$$\begin{cases}
H_0: y[n] = z[n], \\
H_1: y[n] = x[n] + z[n].
\end{cases}$$
(1)

where, y[n] denotes the received signal, z[n] denotes the white Gaussian noise (WGN), and x[n] represents radar signal.

In the context of signal classification, features refer to distinctive signal characteristics that highlight specific phenomena within the signal. We consider that the signals coming from radar are received by M antennas of the base station for a given time slot, as shown in Fig. 3. Our primary focus lies in identifying signal attributes that prove valuable in the detection of radar signals. To formulate the process, first we take absolute values of the time stamps, $|y_i[n]|$ (where, i = 1, 2, ...M) of the same signal. Then we proceed with aggregating them all together for each individual antenna to create a $M \times 1$ dimensional vector, \bar{y} . Next, we generate $M \times M$ covariance matrix, $\bar{y}\bar{y}^H$ for our model which is SPD in nature and can be represented over Riemannian manifold. This is the sample covariance matrix for a given time slot. We repeat the process for all available time slots which provide several points over Riemannian manifold. These points are represented as features to the SVM binary classifier. SVM classifier is trained first then tested to classify H_1 and H_0 .

There are two key probabilities that are essential for assessing detection performance: the probability of false alarm, denoted as $P_{FA} = p(\hat{H}_1|H_0)$, and the probability of detection, represented as $P_D = p(\hat{H}_1|H_1)$. P_{FA} indicates the probability that the classifier incorrectly detects the presence of a radar (\hat{H}_1) when, in reality, no radar exist (H_0) . P_D indicates the probability that the classifier correctly detects the presence of a radar (\hat{H}_1) when radar actually exist (H_1) .

IV. RADAR DETECTION OVER RIEMANNIAN MANIFOLD

Intuitively, received signals at base stations in the presence of incumbent radar should be statistically different from those without radar, thanks to the additional radar-based term x[n] in the received signal model of (1). In other words, second-order statistics (i.e., covariance matrices) of the received signal vary depending on the presence of incumbent radar. We explore the adoption of machine learning approach to tackle radar signal detection. This approach involves training a supervised machine learning model using NIST dataset [15] of waveforms that accurately represent the signals encountered within the CBRS band.

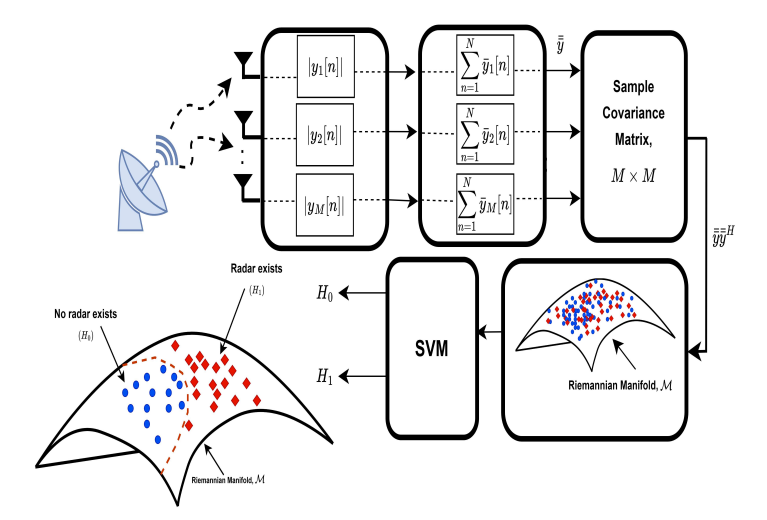


Fig. 3: Block diagram of radar sensing over Riemannian manifold.

Considering (1), we can see that the problem is linked to a two-class classification model where we try to detect the presence of radar utilizing the sample covariance matrices of the received signals. Therefore, we tackle the challenge of identifying incumbent radar signals by framing it as a binary classification problem. In supervised learning, the classifier relies on having accurate labels indicating the presence or absence of radar signals.

The SVM classifier is designed to create an optimal hyperplane for separating two classes. Since in our model, the classes are not linearly separable, we employ the kernel method, which transforms the feature space into a higher-dimensional context. Commonly utilized kernels include linear, polynomial, radial basis function (RBF), and sigmoid [17]. In this work, we assess the detection performance by applying various kernel functions. We analyze the classification accuracy first to select the best kernel function. Then we use the best kernel function for the probability output across a range of SNR values.

Algorithm 1 formalizes the training and testing process of SVM classifier.

V. SIMULATION RESULTS AND DISCUSSION

In this section, we discuss the dataset first, followed by an explanation of the steps and procedures used for training the models and eventually evaluating the performance. These radar waveforms serve as representatives of the signals within the CBRS band. The dataset includes radar signals randomly distributed within a fixed time frame and also the parameters are randomly chosen for each pulse modulation type, intensifying the complexity of the detection task and closely simulating real-world conditions.

Algorithm 1: Training and testing SVM classifier for coexistence scenario over Riemannian manifold

Input: M, total number of base station antennas; T, total number of time slots per antenna; W, total number of waveforms; W_{train} , training set size; C_w , SPD covariance matrix storage

Output: $M_{\text{conf},k}$, confusion matrix.

for $w \in \{1, ..., W\}$ do

1: Take absolute values and aggregate time stamps per antenna having dimension $M \times 1$

2: Calculate covariance matrix C_w of dimension $M \times M$

end

- 3: Prepare features from covariance matrices
- 4: Extract labels corresponding to waveforms
- 5: Standardize features by z-scoring
- 6: Split dataset into training and testing subsets
- 7: Define kernel options

 $K \leftarrow \{\text{'linear'}, \text{'polynomial'}, \text{'rbf'}, \text{'sigmoid'}\}\$

for $k \in K$ do

- 8: Train SVM model SVM_k with kernel k
- 9: Predict test labels with SVM_k
- 10: Compute confusion matrix $M_{\text{conf},k}$

end

11: Compute P_{FA} and P_D .

A. NIST Dataset

To build our model, we rely on synthetically generated NIST dataset [15]. The dataset offers numerous waveforms, each lasting 80 milliseconds, presented as pairs of I and Q values. We use 800,000 time stamps for each of these waveforms. Also, these waveforms are associated with a 10 MHz band. Approximately half of these waveforms solely represent receiver noise without any radar signal, while the remaining waveforms include radar signals. Based on their characteristics, five distinct radar types are categorized in the dataset determined by their pulse modulation and parameter ranges. These categories are referred to as waveform bins. Each bin encompasses a specific range of parameters that represent various radar designs within the 3.5 GHz CBRS band, both existing and anticipated in the future. Among the waveforms that contain radar signals, each may have at most one radar signal, randomly selected from the five radar types. In addition, the radar signals are placed at randomly chosen times within the fixed duration which makes the detection problem more challenging and closer to real-world scenarios. Furthermore, the Signal-to-Noise Ratio (SNR) of these radar signals is randomly chosen from the range of [10, 12, 14, 16, 18, 20] dB. In both the training and testing phases, we apply Zscore normalization, a method that standardizes feature values

to possess an average of 0 and a standard deviation of 1. This process involves subtracting the feature's mean from each value and subsequently dividing by the standard deviation.

B. Classifier Training

A total of 4000 waveforms are employed for training, evenly divided into two categories: one half comprises radar signals, while the other consists solely of noise. For the purpose of training our model with each considered SNR value, we select 200 waveforms, ensuring an equal distribution of radar and noise-only signals. To prevent any potential bias stemming from data order, we randomize the sequence of these waveforms. Subsequently, we utilize 50% of these randomized waveform samples for the training process.

C. Evaluating Detection Performance

We use the trained SVM model to test rest of the 50% waveform samples for different kernel types. We first check the overall classification accuracy of the model combined across all SNR values and all radar types. Then we verify the radar detection accuracy and false alarm rate individually against the SVM kernel which has the best classification accuracy.

- 1) Classification Accuracy: This accuracy metric reflects the overall ability of the model to correctly classify instances as either radar or non-radar. Classification accuracy is the proportion of true results (both true positives and true negatives) among the total number of cases examined. Following is the list of different performance measuring terms:
 - True positive (TP): Radar signals correctly identified as radar.
 - True negative (TN): Non-radar signals correctly identified as non-radar.
 - False positive (FP): Non-radar signals incorrectly identified as radar.
 - False negative (FN): Radar signals incorrectly identified as non-radar.

We calculate the classification accuracy (CA) as

$$CA = \frac{TP + TN}{TP + TN + FP + FN} \tag{2}$$

Table I represents the classification accuracy of different SVM kernel functions. Although, sigmoid function give a good classification accuracy of 86.54%, RBF kernel has the best classification accuracy than rest of the functions with 87% accuracy. This performance metric measures how often the classifier is correct.

2) Detection under various SNR: In Figure 4, we present the detection rate and false positive rate across various SNR values. The true positive rate, or detection rate, is represented on the left y-axis, while the false positive rate, or probability of false alarm, is depicted on the right y-axis. Since, RBF kernel

TABLE I: Classification Accuracy of SVM Kernels

Kernel Type	Classification Accuracy (%)
Linear	83.89
Polynomial	83.06
Sigmoid	86.54
RBF	87.00

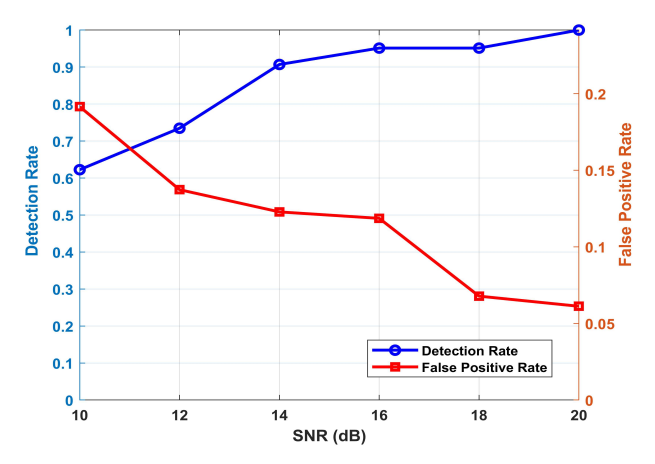


Fig. 4: SNR versus detection rate and false positive rate for SVM with Gaussian (RBF) kernel

TABLE II: Performance metrics of SVM with RBF kernel

SNR	Recall	Precision	F1-score
10	0.79	0.62	0.69
12	0.84	0.73	0.78
14	0.85	0.91	0.88
16	0.85	0.95	0.90
18	0.91	0.95	0.93
20	0.93	1	0.96

showcase best classification accuracy, we evaluate our data using RBF kernel. Notably, RBF kernel achieves a detection accuracy of over 90% and the lowest false positive rate up to an SNR of 14 dB. For the case of spectrum sharing, false negative rate is also a vital parameter as it determines the instances when the model incorrectly identifies radar signals as non-radar signal. RBF kernel maintains less than 9% false negative rate up to 14 dB SNR in our proposed model. Given the complexity of the dataset, achieving such a high level of accuracy is not assured by alternative methods of a similar kind.

Performance metrics like recall, precision, and F1-score are crucial for evaluating the performance of any classification model. The recall, precision, and F1-score can be expressed as follows

$$Recall = \frac{TP}{TP + FN}$$
 (3)

$$Precision = \frac{TP}{TP + FP}$$
 (4)

TABLE III: Confusion Matrices for SVM with RBF kernel

	Predicted	
	Positive	Negative
Actual Positive	44.00%	12.33%
	(TP)	(FN)
Actual Negative	7.67%	36.00%
	(FP)	(TN)

a) SNR range in [10, 14] dB

	Predicted	
	Positive	Negative
Actual Positive	52.94%	1.38%
	(TP)	(FN)
Actual Negative	4.84%	40.83%
	(FP)	(TN)

b) SNR range in [16, 20] dB

$$F1\text{-Score} = \frac{2 \times Precision \times Recall}{Precision + Recall}$$
 (5)

High recall value indicates that the model is good at identifying all actual positive cases which also means it hardly misses the positive cases (i.e., a low number of false negatives), whereas high precision means a low false positive rate, and a high F1 score indicates a balance between precision and recall, signifying a model that performs well both in correctly identifying positive instances and in minimizing false positives. The results illustrated in Table II show the recall, precision, and F1-score (weighted average of the precision and recall) for our model of SVM classifier with RBF kernel. It is seen that the SVM classifier with RBF kernel function maintains a precision of above 0.90 up to 14 dB SNR and then it starts to decrease with decreasing SNR.

Finally, Table III presents a comparison of accuracy results between the testing dataset with higher SNR (SNR range in [16, 20] dB) and the lower SNR (SNR range in [10, 14] dB) when employing the RBF kernel. With a decrease in the SNR range, we observe a decline in overall accuracy from 93.77% to 80% and an increase in overall false prediction from 6.22% to 20%.

VI. CONCLUSION

In this paper, we present a novel coexistence scenario modeled over Riemannian manifold. Such modeling includes reception of waveforms by each of the antennas and utilization of their covariance matrices to ensure feature extraction in simplified way from a dataset which is relatively challenging and close to the real-world scenario. Our main objective is to detect radar signals at the base station to employ on-demand spectrum access strategies. In the decentralized mode, this

process will enable the base station to decide whether to use a shared band like CBRS with radars or not. As a supervised machine learning technique, we use support vector machine (SVM) with different kernel functions to serve as the classifier between two classes of consideration. Results verify that SVM with RBF kernel maintains more than 90% radar detection accuracy for SNR value up to 14 dB along with comparatively lower false alarm rate. Furthermore, we evaluate other essential performance metrics like recall, precision, and F1-score for the RBF kernel. These metrics also verify the robustness of the model.

REFERENCES

- S. Sarkar, D. Guo, and D. Cabric, "RadYOLOLet: Radar Detection and Parameter Estimation Using YOLO and WaveLet," arXiv preprint arXiv:2309.12094, 2023.
- [2] F. H. Sanders, "Procedures For Laboratory Testing of Environmental Sensing Capability Sensor Devices," Institute for Telecommunication Sciences, Tech. Rep., 2017.
- [3] R. Caromi, M. Souryal, and W.-B. Yang, "Detection of Incumbent Radar in the 3.5 GHZ CBRS Band," in 2018 IEEE Global Conference on Signal and Information Processing (GlobalSIP), 2018, pp. 241–245.
- [4] R. Caromi, A. Lackpour, K. Kallas, T. Nguyen, and M. Souryal, "Deep Learning for Radar Signal Detection in the 3.5 GHz CBRS Band," in 2021 IEEE International Symposium on Dynamic Spectrum Access Networks (DySPAN), 2021, pp. 1–8.
- [5] W. M. Lees, A. Wunderlich, P. J. Jeavons, P. D. Hale, and M. R. Souryal, "Deep Learning Classification of 3.5-GHz Band Spectrograms With Applications to Spectrum Sensing," *IEEE Transactions on Cognitive Communications and Networking*, vol. 5, no. 2, pp. 224–236, 2019.
- [6] A. Selim, F. Paisana, J. A. Arokkiam, Y. Zhang, L. Doyle, and L. A. DaSilva, "Spectrum Monitoring for Radar Bands Using Deep Convolutional Neural Networks," in GLOBECOM 2017 2017 IEEE Global Communications Conference, 2017, pp. 1–6.

- [7] S. Sarkar, M. Buddhikot, A. Baset, and S. K. Kasera, "DeepRadar: A Deep-Learning-based Environmental Sensing Capability Sensor Design for CBRS," in *Proceedings of the 27th Annual International Conference* on Mobile Computing and Networking, 2021, pp. 56–68.
- [8] I. Nasim and A. S. Ibrahim, "Millimeter Wave Beamforming Codebook Design via Learning Channel Covariance Matrices Over Riemannian Manifolds," *IEEE Access*, vol. 10, pp. 119617–119629, 2022.
- [9] J. J. Sadique, I. Nasim, and A. S. Ibrahim, "Covariance Shaping Over Riemannian Manifolds for Massive MIMO Communication," *IEEE Access*, vol. 11, pp. 142 874–142 883, 2023.
- [10] R. Shelim and A. S. Ibrahim, "Wireless Link Scheduling Over Recurrent Riemannian Manifolds," *IEEE Transactions on Vehicular Technology*, vol. 72, no. 4, pp. 4959–4968, 2023.
- [11] A. S. Ibrahim, "Wireless Link Scheduling via Interference-aware Symmetric Positive Definite Connectivity Manifolds," in 2021 IEEE International Conference on Communications Workshops (ICC Workshops), 2021, pp. 1–5.
- [12] Q. Chen, P. Wan, Y. Wang, J. Li, and Y. Xiao, "Research on cognitive radio spectrum sensing method based on information geometry," in *Cloud Computing and Security*, X. Sun, H.-C. Chao, X. You, and E. Bertino, Eds. Cham: Springer International Publishing, 2017, pp. 554–564.
- [13] Q. Lu, S. Yang, and F. Liu, "Wideband Spectrum Sensing Based on Riemannian Distance for Cognitive Radio Networks," Sensors, vol. 17, no. 4, 2017. [Online]. Available: https://www.mdpi.com/1424-8220/17/4/661
- [14] S. Zhang, Y. Wang, Y. Zhang, P. Wan, and J. Zhuang, "A Novel Clustering Algorithm Based on Information Geometry for Cooperative Spectrum Sensing," *IEEE Systems Journal*, vol. 15, no. 2, pp. 3121–3130, 2021
- [15] R. Caromi, M. Souryal, and T. A. Hall, "RF Dataset of Incumbent Radar Signals in the 3.5 GHz CBRS Band," *Journal of Research of the National Institute of Standards and Technology*, vol. 124, p. 1, 2019.
- [16] J. M. Lee, Introduction to Riemannian Manifolds. Springer, 2018, vol. 2.
- [17] P. Tsangaratos and I. Ilia, "Applying Machine Learning Algorithms in Landslide Susceptibility Assessments," in *Handbook of Neural Computation*. Elsevier, 2017, pp. 433–457.